Spatial Interception for Mobile Robots

Anthony Suluh, Keshav Mundhra, Thomas Sugar, Michael McBeath

Mechanical and Aerospace Engineering, Psychology
Arizona State University
Tempe, AZ 85283

Abstract

Human based vision algorithms for interception of fly balls in one-dimension have been researched and studied. We are developing new perceptual strategies for three-dimensional space that are robust and simple. Results from simulations have shown the feasibility of human vision algorithms for catching. This paper discusses the experimental validation of two perceptual algorithms: Linear Optical Trajectory (LOT) and the Optical Acceleration Cancellation (OAC).

1 Introduction

Different spatial perception strategies for intercepting a projectile have been debated. These strategies are used to determine a path that allows the fielder to converge to the destination of the projectile. The strategies assume that humans have a low-level unconscious visual-motor control algorithm that is reliable and robust.

One strategy, the 3D OAC model describes the fielder catching a fly ball by selecting a running path, which achieves a constant optical rate in the image plane. The fielder runs along a path that horizontally maintains his alignment with the ball while maintaining a constant change in the tangent of the optical angle.

Another perceptual strategy is the LOT proposed by McBeath et al. [1]. The LOT strategy maintains the optical projection angle ψ to be constant. See Figure 1. By doing so, the image of the ball always rises above the fielder guaranteeing that the fielder travels to the correct destination.

In the present work, experiments are conducted to validate the 3D OAC and the LOT models and to demonstrate the behavior of human based visual-servoing in robotics. The advantages to these strategies are twofold. Firstly, these strategies describe a path for a projectile that can move in three dimensions. Secondly, they use only optical geometry and time to compute a fielder's path to intercept an object, thus, avoiding complex dynamic analysis.

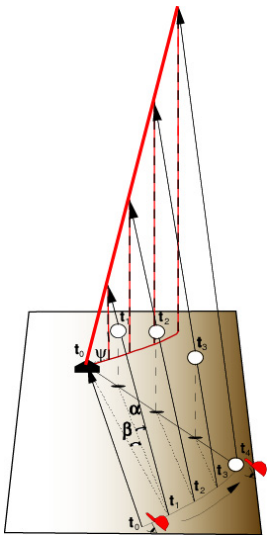

Figure 1: Linear Optical Trajectory strategy maintains a linear optical ball trajectory on the background scenery. Fielders adjust their path to keep the image of the ball on the projection plane monotonically rising along the straight-line trajectory described by the angle, ψ.

2 Literature Review

There are two perceptual models proposed to explain catching in 3D. The 3D OAC model states that the fielder chooses a running path that is laterally aligned with the ball and his velocity is adjusted so that the rate of change of the tangent of the vertical optical angle, $\tan(\alpha)$, is constant with respect to time [2, 3]. If the rate of change of $\tan(\alpha)$ increases, the fielder has run too far forward (or too slowly backward). Similarly, if the rate of change of $\tan(\alpha)$ decreases, the fielder has run too far backwards. The second model, the LOT, proposes that the fielder maintains a linear optical trajectory of the ball [1]. The LOT model maintains a constant optical projection angle so that there exists an imaginary line on the background scenery due to the projection of the image of the ball, as viewed by the fielder.

In 1994, Oudejans, Michaels and Bakker proposed that the catchableness depends on the locomotory ca-

pabilities such as speed and acceleration of the fielder rather than pure body scaling [4]. Their specification of catchableness of a fly ball on the basis of vertical optical acceleration occurs when the optical acceleration is zero at a certain moment. This informs the catcher that the ball is catchable, assuming that the fielder is capable of maintaining the current running speed. Optical acceleration is not just about a ball trajectory or about action of the fielders, but a combination of both. In another study, they concluded that the information source for guidance of locomotion in the direction of the ball is not detected from the motion of the ball on the retina [5], but is detected by head and eye motion.

In robotics, Burgstadt and Ferrier have demonstrated a mobile robot based on the OAC strategy [6]. In our previous work, we developed perceptual algorithms in the visual plane for 2D passive and active OAC. In passive OAC, the camera is always stationary (no tilting) and the robot moves to keep the image constantly rising on the image plane. In active OAC, however, the tilt of the camera is constantly adjusted according to the rate at which the center of the ball moves in the image plane, and the robot moves to maintain the ball at the center of the image [3, 7, 8].

This paper will first describe the 3D OAC and LOT mathematically and provide simulations. Next, experimental data from the robot is presented and discussed in Section 4.

3 Mathematical Modeling and Simulation

3.1 OAC Model in 3 Dimension (OAC 3D)

The fixed global coordinate system is rotated about the home plate (See Figure 2) and the fielder is modeled as a particle moving in a 2D plane to simplify the calculations. When the robot initially looks at the ball, it will align the camera, and the coordinate system will be rotated by an amount

$$\theta = \tan^{-1}\left(\frac{(y_{fi} - y_{bi})}{(x_{fi} - x_{bi})}\right). \tag{1}$$

This new coordinate system will be fixed during the entire interception task. For example, in the new coordinate system, the robot's position will be adjusted in order to keep the CCD image of the ball constantly rising in the x' direction and keep the image of the ball centered in the y' direction. If the robot rotates during the interception task, the camera will be panned in the opposite direction to keep the orientation of the camera fixed during the entire task. It is important to note that experimentally, the ball will rise in the CCD image plane and the fielder will not calculate or know the exact global position of the ball. For simulation purposes, the following equations are derived for the OAC model.

$$\tan\alpha = C't \tag{2}$$

$$x'_f = x'_b + \frac{z'_b}{C't} \tag{3}$$

$$y'_f = y'_b. \tag{4}$$

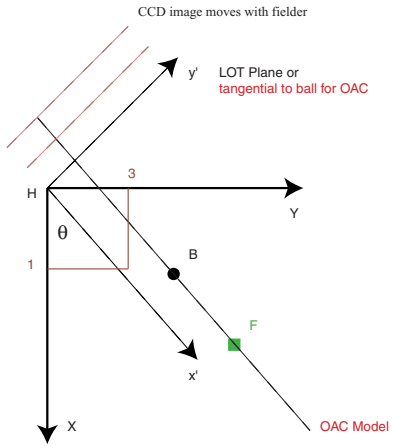

Figure 2: The fixed, global coordinate system is rotated by an angle θ to make the calculations much simpler. In the the new (x', y') coordinate system, the x' axis is initially aligned with the ball and the robot. Fielders maintain the lateral alignment in the y' direction. As the fielders move forward or backward based on the OAC strategy in the x' direction, the image plane is also allowed to move accordingly so that the distance between the fielder and the image plane is always constant.

The height of the ball is calculated in the plane that passes through the y' axis ($z_{imageOAC}$) or in the plane that moves (forward or backward) with the fielder (z_{ccdOAC}). The moving plane is always orthogonal to the x' axis. See Figure 2.

$$z_{imageOAC} = x'_f C't \tag{5}$$

$$z_{ccdOAC} = x'_f(0)C't = A(constant)t \tag{6}$$

$$C' = \frac{z'_b(0.3s)}{0.3(x'_f(0.3) - x'_b(0.3))} \tag{7}$$

The constant C' is calculated just after the ball starts on its motion. We chose to use a value of 0.3 seconds corresponding to 4 frames. A proportional controller is used to adjust the robot's position. The equations for the robot velocities in x' and y' directions are derived.

$$\dot{x}'_f = K_{px}\left(\left(\frac{z_b}{x'_f - y'_b}\right)D - at\right) \tag{8}$$

$$\dot{y}'_f = K_{py}(y'_f - y'_b) \tag{9}$$

3.2 Fixed LOT and Moving LOT Model

Aboufadel developed a mathematical description of the LOT model in world coordinates [9], but it is very complicated because a rotated coordinate system was not used. In the rotated coordinate frame, the LOT image plane (vertical plane) is aligned with the y' axis. The robot adjusts its position to keep the image of the ball monotonically rising along the vector described by the angle ψ, which lies on the LOT image plane. In this analysis, the LOT image plane does not move forward or backward. It is fixed.

$$\tan\psi = C_2' \quad (10)$$

$$x_f' = \frac{C_2' x_b'}{C_2' - \frac{z_b'}{y_b'}} \quad (11)$$

$$y_f' = y_b' \quad (12)$$

$$C_2' = \frac{z_b'(0.3)x_f'(0.3)}{y_b'(0.3)(x_f'(0.3) - x_b'(0.3))} \quad (13)$$

$$z_{imageLOT} = x_f' \tan(\alpha) \quad (14)$$

$$z_{ccdLOT} = x_f'(0)\tan(\alpha) \quad (15)$$

The same proportional controller is used to control the robot based on the fixed LOT strategy.

$$\dot{x}_f' = K_{px}\left(\left(\frac{z_b}{x_f' - y_b'}\right)x_f' - y_b' C_2'\right) \quad (16)$$

$$\dot{y}_f' = K_{py}(y_f' - y_b') \quad (17)$$

It is important to note that time does not appear in the equations for the LOT model. Also, if the ball is hit directly at the fielder, the LOT model breaks down due to a singularity. The height of the ball in the fixed image plane is given by $z_{imageLOT}$. The height of the ball in the CCD-image plane that moves with the fielder is given for reference purposes.

The LOT algorithm is different if the fielder keeps the ball moving in a straight line in the moving image plane. As the fielder moves forward or backward, the image plane moves keeping a fixed distance D from the fielder. The constraint is due to the constant focal distance of the camera. The controller for the moving LOT algorithm (more realistic) is shown below.

$$\tan\psi = C_2' \quad (18)$$

$$x_f' = x_b' + \frac{D z_b'}{C_2' y_b'} \quad (19)$$

$$y_f' = y_b' \quad (20)$$

$$D = x_f'(0) \quad (21)$$

$$z_{movingccdLOT} = D\tan(\alpha) \quad (22)$$

$$\dot{x}_f' = K_{px}\left(\left(\frac{z_b}{x_f' - y_b'}\right)D - y_b' C_2'\right) \quad (23)$$

$$\dot{y}_f' = K_{py}(y_f' - y_b') \quad (24)$$

3.3 Simulation

Because the robot has nonholonomic constraints, a non-linear look-ahead controller is used. The velocities obtained from above equations are substituted into the look ahead-controller to determine the translational velocity and the angular velocity of the robot,

$$\begin{pmatrix} v \\ \dot{\theta} \end{pmatrix} = \begin{bmatrix} \cos(\theta) & \sin(\theta) \\ -\sin(\theta)/l & \cos(\theta)/l \end{bmatrix} \begin{pmatrix} \dot{x}_f' \\ \dot{y}_f' \end{pmatrix} \quad (25)$$

where l is the look ahead distance from the center of the robot.

In these simulations, the ball trajectory is $x_b = 75t$, $y_b = 10t$, and $z_b = -64t^2 + 256t$. The fielder's initial position is $x_f = 270$ and $y_f = 70$. The constants, C' and C_2', are calculated in the rotated frame at $0.3s$ right after the ball is hit, and remain fixed.

The ball trajectory, as well as the fielder's trajectory are shown in Figure 3. The ball and fielder's trajectories are projected in the (x,y) plane. See Figure 4. Different initial positions for the fielder are explored and shown in Figure 5. The OAC and moving LOT models determine straighter paths.

The ball trajectory is first rotated into the (x', y') frame and then the algorithm is used to calculate the fielder's trajectory. All data is then rotated back to the original (x, y) coordinate system for the purpose of presentation.

In the next simulation, wind is introduced and the ball trajectory is no longer a perfect parabola. The fielder takes an initial look at the ball after 0.3 sec and the values for C' and C_2' are used throughout the simulation, even though the path of the ball changes. The altered ball trajectory and different fielder's trajectories are projected in the (x,y) plane and are shown in Figure 6.

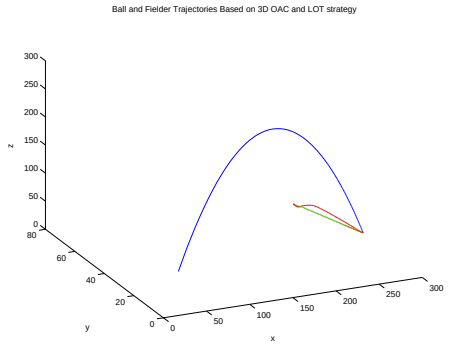

Figure 3: The ball and the fielder's trajectories are shown.

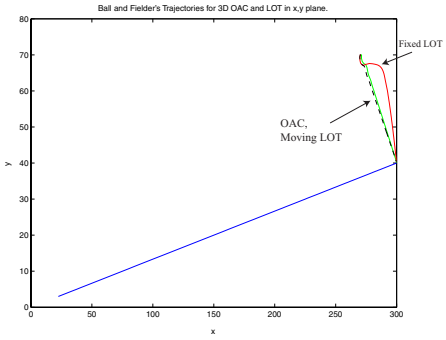

Figure 4: The ball and the fielder's trajectories: the OAC (green), the Moving LOT (dotted black), and the Fixed LOT (red) are projected in the (x, y) plane. The OAC and the Moving LOT algorithms determine a straight path to the destination. The Fixed LOT (red) shows a curved path.

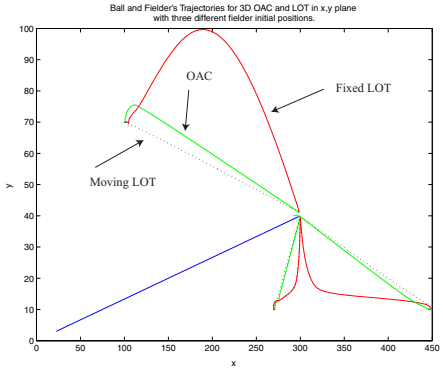

Figure 5: The ball and the fielder's trajectories: the OAC (green), the Moving LOT (dotted black), and the Fixed LOT (red) are projected in the (x, y) plane. The three initial fielder's positions are (270,10), (450,10) and (100,70). The ball is intercepted with different starting points.

4 Experiment

4.1 Set Up

A Nomad Super Scout from Nomadic Technologies Inc. with an additional pan-tilt mechanism from Direct Perception is used. The computer on the robot runs Linux as the operating system and controls the drive wheels, the pan-tilt and the PCI frame grabber. The code is written in the C language. The center of mass of the balloon is obtained from a standard calculation.

4.2 Validation

If the balloon moves in a perfect parabolic trajectory, a unique case, then both the OAC and the Moving LOT describe similar paths. The image of the center of the balloon captured by a stationary robot

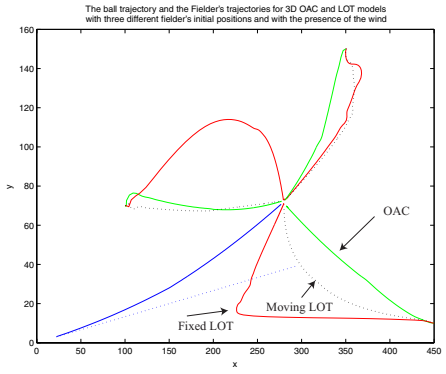

Figure 6: The ball and the fielder's trajectories: the OAC (green), the Moving LOT (dotted black), and the Fixed LOT (red) are projected in the (x, y) plane. The three initial fielder's positions are (450,10), (350,150) and (100,70). The wind causes all paths to deviate, but the ball is intercepted.

at an ideal position follows a linear trajectory, which agrees with the LOT strategy. See Figure 7. Moreover, the increment of the center of the balloon in the vertical direction in the image plane is constant which agrees with the OAC strategy. See Figure 8. In this unique case, it is concluded that the image trajectory moves in a straight line and also rises at a constant rate.

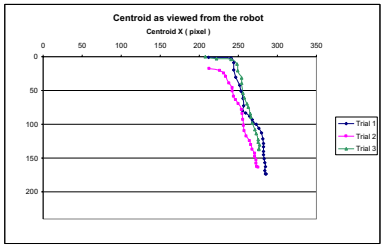

Figure 7: The center of the balloon on the image plane captured by a stationary robot at the the ideal interception point. The trajectory follows a linear path that satisfies the LOT model.

4.3 Experiment 1, 3D Active OAC Model

In this experiment, we implement the 3-D active OAC Model described earlier in the paper. During the initial motion of the balloon, the camera is panned so that the image of the balloon is approximately in the center of the view. This motion is analyzed to obtain the rate at which the center of the balloon rises, and the camera is actively tilted at this rate during the entire task. The robot is programmed using the active control algorithm which keeps the desired position of the balloon always at the center of the image [4]. As the robot rotates in a certain direction, the camera is

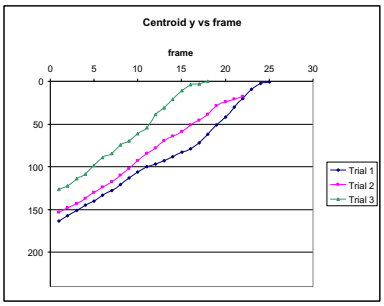

Figure 8: The height of balloon in the y direction rises linearly on the image plane which satisfies the OAC strategy.

panned in the opposite direction to keep the orientation of the y' plane fixed.

In the first trial, the balloon travels in a parabolic path such that it heads in front and to the right of the robot. At the start of the experiment, the center of the balloon is very close to the desired center in the x' direction, thus the angular velocity of the robot is small. See Figures 9 and 10. Also, at the start, the center of the balloon is above the desired center by 80 pixels in the y' direction. This causes the robot to accelerate backward. As the robot moves back and the camera is tilted up at a constant rate, the actual center of the balloon in the image drops to the right of the robot causing it to slow down and start turning right. Once the image of the balloon is below the desired center, the robot starts accelerating forward while maintaining the lateral alignment with the balloon in the fixed y' plane.

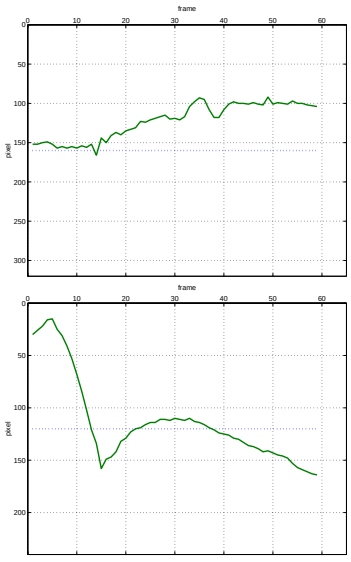

Figure 9: The centroid of the balloon in the x direction (top) and the centroid of the balloon in the y direction (bottom). Case 1.

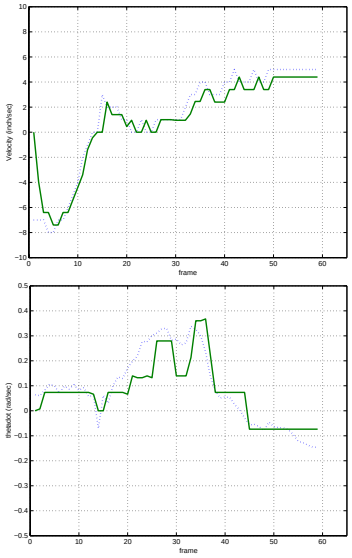

Figure 10: Translational velocity of the robot (top) and the angular velocity of the robot (bottom).

In the second trial, the balloon moves in a parabolic path such that it heads behind and to the right of the robot. See Figure 11.

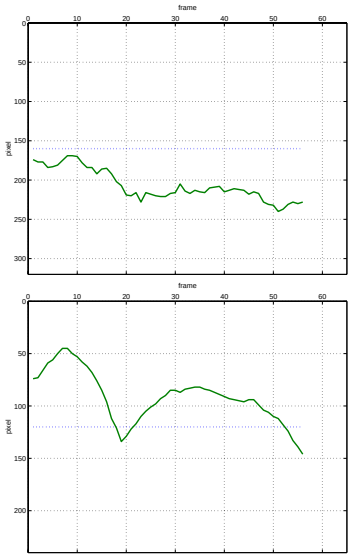

Figure 11: The centroid of the balloon in the x direction (top) and the centroid of the balloon in the y direction (bottom). Case 2.

4.4 Experiment 2, LOT

In the LOT strategy, the trajectory of the balloon in the image plane follows a straight line. In the first few frames, the robot calculates the rates at which the center of the balloon moves horizontally and vertically. The camera is panned and tilted with the same rates

and the robot moves to maintain the balloon at the center of the image. Because the focal distance of the camera is not changed, the second LOT strategy (moving LOT) is employed. In the first case, the balloon heads in front of the robot. See Figure 12.

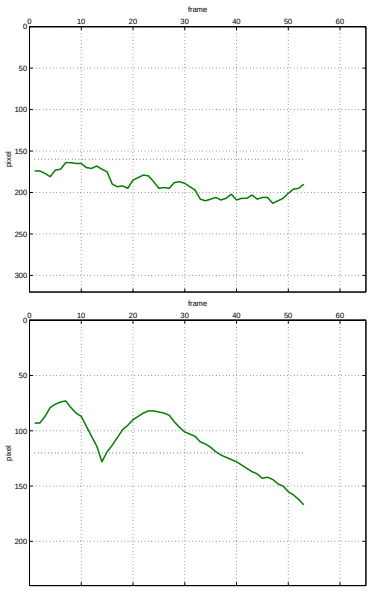

Figure 12: The centroid of the balloon in the x direction (top) and the centroid of the balloon in the y direction (bottom). Case 1.

In the second experiment, the balloon heads behind and to the right of the robot. In this case, the robot first moves backward and also turns so that the image of the balloon is always in the view of the robot. See Figure 13.

5 Conclusion

We are investigating perceptual principles such as constant image rate (OAC), and angular constancy in the image plane (LOT), and applying these principles to navigational pursuit. With these principles, control algorithms for visual-servoing will allow mobile robots to intercept projectiles with complicated and varying trajectories. We developed algorithms using both the OAC and the LOT models proposed by psychologists in three dimensions.

The OAC algorithm implemented on the robot is capable of maintaining the lateral error between the ball and the robot close to zero, and is able to move backward or forward to cancel the optical acceleration. The LOT strategy keeps the position of the ball straight in the image plane using only geometric data, and it also maintain the lateral error between the ball and the robot close to zero.

In the simulation with a perfect parabolic trajectory, the image of the ball not only rises at a constant rate on the image plane but also the position of the ball on the moving image plane follows a straight line. We believe the multi-disciplinary research between perceptual psychology and robotics will help us develop navigational algorithms that will be robust, powerful, and simple.

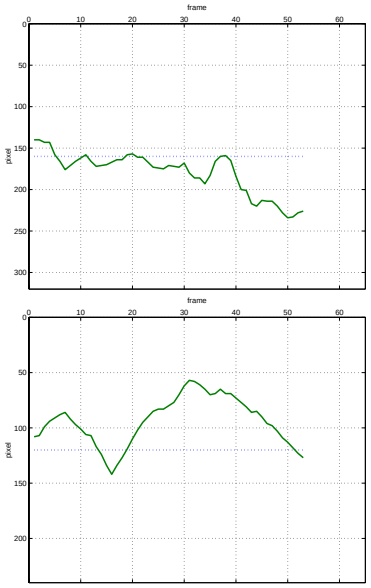

Figure 13: The centroid of the balloon in the x direction (top) and the centroid of the balloon in the y direction (bottom). Case 2.

References

[1] M. K. McBeath, D. M. Shaffer, and M. K. Kaiser, "How baseball outfielders determine where to run to catch fly balls," *Science*, vol. 268, no. 5210, pp. 569–573, 1995.

[2] P. McLeod and Z. Dienes, "Running to catch the ball," *Nature*, vol. 362, no. 6415, 1993.

[3] T. Sugar and M. McBeath, "Spatial navigational algorithms: Applications to mobile robotics," in *Vision Interface, VI 2001*, 2001.

[4] R. R. D. Oudejans, C. F. Michaels, F. C. Bakker, and A. Dolne, "The relevance of action in perceiving affordances : Perception of catchableness of fly balls," *Journal of Experimental Psychology: Human Perception and Performance*, vol. 22, no. 4, pp. 879–891, 1996.

[5] R. R. D. Oudejans, C. F. Michaels, F. C. Bakker, A. Dolne, and K. Davids, "Shedding some light on catching in the dark: Perceptual mechanism for catching fly balls," *Journal of Experimental Psychology: Human Perception and Performance*, vol. 25, no. 2, pp. 531–542, 1999.

[6] J. A. Borgstadt and N. J. Ferrier, "Interception of a projectile using a human vision-based strategy," in *IEEE International Conference on Robotics and Automation*, 2000.

[7] A. Suluh, T. Sugar, and M. McBeath, "Spatial navigational principles: Applications to mobile robotics," in *IEEE International Conference on Robotics and Automation*, 2001.

[8] M. McBeath, T. Sugar, and D. Shaffer, "Comparison of active versus passive ball catching control algorithms using robotic simulations," in *Vision Sciences Conference*, 2001.

[9] E. Aboufadel, "A mathematician catches a baseball," *American Mathematics Monitor*, vol. 103, pp. 870–878, 1996.